EPJ Web of Conferences **94**, 02005 (2015)
DOI: 10.1051/epjconf/20159402005

Characterization of the dynamic behaviour of ALGOTUF armour steel during impact and in torsion

Nabil Bassim[1,a], Solomon Boakye-Yiadom[1], Genevieve Toussaint[2], and Manon Bolduc[2]

[1] Department of Mechanical Engineering, University of Manitoba, Winnipeg, Canada
[2] DRDC Valcatier, Department of National Defense, Quebec, Canada

Abstract. Algotuf is a new steel which is proposed as a candidate for armour material. To assess this application, a study of the impact properties of this steel was conducted at the University of Manitoba using two types of Hopkinson Bar systems, namely a torsional bar equipment and a direct impact system capable of producing high strain rates and large strains. Stress strain curves for the steels were obtained in pure shear and in compression. Temperatures of 25 °C, 200 °C and 500 °C were used in the testing. Following the testing, a microstructural examination of the specimens tested was carried out to investigate the effect of microstructure on the mechanism of failure of this material. It was found that, above a value of impact momentum corresponding to a high strain rate, adiabatic shear bands are formed. The microscopic examination showed that the initiation of these shear bands corresponded at locations where martensitic laths were present and around regions of maximum shear stresses. Generally, the shear bands act as precursors to the formation of microcracks that may lead to failure. On the other hand, the high strength and formability of the steel makes it suitable for use as an armour material.

1. Introduction

The behavior of materials and their mechanical properties at high strain rates of deformation differ considerably from that observed at quasi-static or intermediate strain rates. Deformation of materials at quasi-static or intermediate strain rates is characterized by slip and twinning mechanisms [1,2]. However, at high strain rates such as impact, explosive forming, and ballistics, plastic deformation is characterized by strain localization along narrow bands [3,4]. This results in crack nucleation and propagation and subsequent fracture and fragmentation.

In this study, two types of Hopkinson Bar systems, namely a torsional bar equipment and a direct impact system were used to test Algotuf steel specimens at room temperature (25 °C), and at high temperatures of 200 °C and 500 °C. Following the testing, a microstructural examination of the specimens tested was carried out to investigate the effect of dynamic deformation and testing temperature on the mechanism of failure of this material.

2. Experimental procedures

2.1. Dynamic Torsion Tests of Algotuf

High strain rate torsion tests were conducted on Algotuf specimens using a Torsional Split Hopkinson Bar (TSHB) under room and high temperature conditions. Specimens were cut from received plates and machined to specifications. The specimens were grouped and tested under room temperature, at 200 °C and 500 °C using the TSHB. The test specimens were thin-walled tubes with a thickness of 0.4 and a length of 3.8 mm. Details of the testing procedure are provided in [5,6]. The torque needed to rapidly load the specimen is determined by the angle of twist and stored in the loading end of the input bar [6]. When the loading arm is released, an elastic wave is generated which travels rapidly through the input bar and is recorded as incident wave by attached strain gages. Part of this incident wave is used in deforming the specimen and part is transmitted through the specimen on to the output bar as transmitted wave. The transmitted wave is captured by the strain gage attached to the output bar. The fraction of the elastic wave that was used in deforming the specimen is reflected back and captured by the strain gage attached to the input bar as reflected wave. These three waves provide the strain signals which are conditioned, amplified and recorded by the data acquisition system connected to the bars. Dynamic stress-strain curves are generated from the captured strain wave signals.

2.2. Dynamic impact tests of Algotuf

High strain rate compression tests were conducted on the Algotuf steel specimens using a Direct Impact Hopkinson Pressure Bar (DIHPB). Cylindrical test specimens (10.5 × 9.5 mm) were impacted using a 1.905 kg quench-hardened AISI 4340 steel bar projectile. The projectile travels through a light gun barrel and strikes the test specimen attached to the output bar of the Hopkinson bar system. The output bar is also made from quench-hardened AISI 4340 steel with the same cross-sectional area as the striking projectile. The elastic waves generated when the specimen is impacted travels through the output bar and is captured by strain gage attached to it. This provides the strain signals which are conditioned, amplified and captured by the data acquisition system connected to the bar. The data acquisition system consists of strain pulse conditioner/amplifier and a mixed signal digital

[a] Corresponding author: bassimnabil@hotmail.com

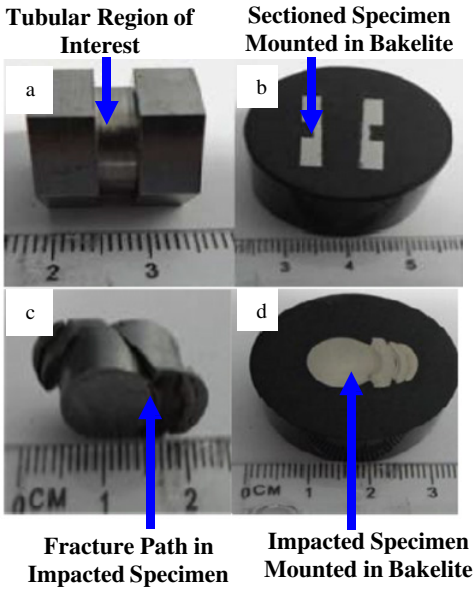

Figure 1. Images of the deformed (a), (b) torsional (c), (d) impacted Algotuf specimens showing the regions where microstructural analyses were carried out.

oscilloscope. Dynamic stress-strain curves are generated from the captured strain signals.

2.3. Metallographic analysis

Metallographic and electron microscopy (SEM) analysis of the deformed specimens were carried out to determine the effect of dynamic deformation and testing temperature on the mechanism of failure of this material. Selected deformed specimens were cut, grinded, polished, and etched with a 2% Nital solution. Micro- hardness measurements were performed with a Buehler micromet 5100 series under a test load of 300 gf. Microstructural investigations were carried out with an inverted reflected light optical microscope (OM) equipped with a CLEMEX vision image analyzer and a JSM 5900 scanning electron microscope (SEM) with an Oxford EDS system. Figure 1 shows the steel specimens after torsional and impact tests as well as the mounted specimens where the microstructural analyses were done.

3. Results

3.1. Results of dynamic torsion tests

Figure 2 shows the true shear stress vrs shear strain graphs for specimens all deformed at 6° angle of twist at Room Temperature (RT), and at High Temperstures (HT) of 200 °C and 500 °C. In general, shear stress increases initially with increasing shear strain, reaches a maximum and decreases with subsequent increase in shear strain irrespective of the testing temperature. The average strain rates increased as the testing temperature increase. The average strain rate was 580 S^{-1} for the steel specimens tested at 6 ° angle of twist at room temperature. At the same angle of twist, the average strain rates increased to 638 S^{-1} for the specimens tested at 200 °C and 702 S^{-1} at 500 °C.

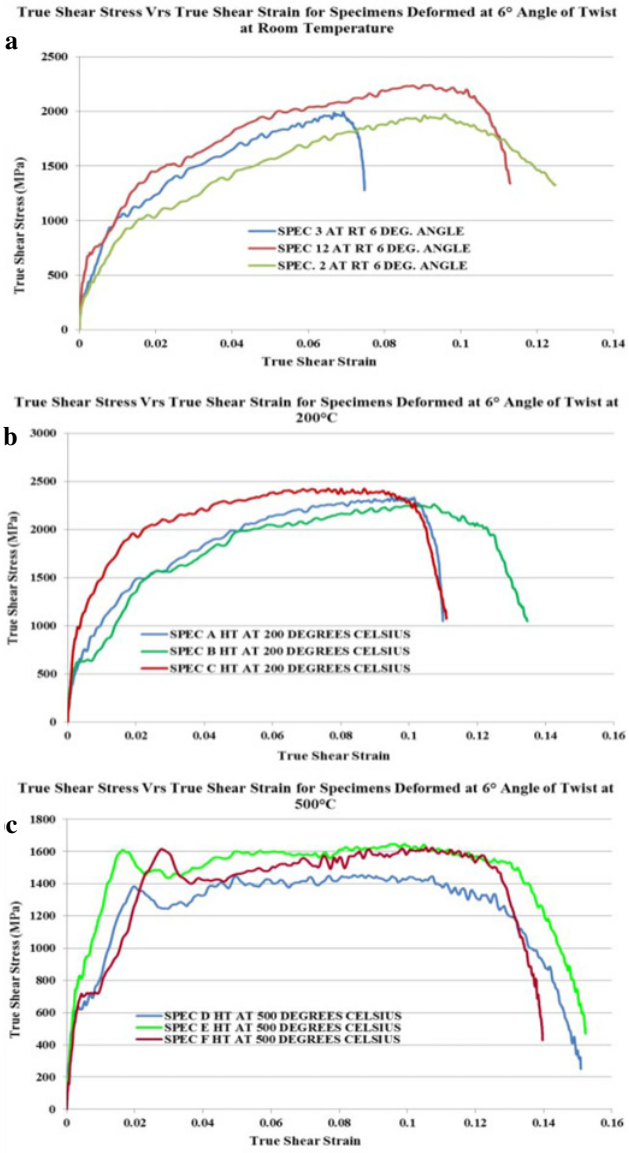

Figure 2. True shear stress – shear strain graphs for specimens all deformed at 6° angle of twist at (a) Room Temperature (RT), (b) 200 °C and (c) 500 °C.

Table 1 shows the strain rates and maximum shear stresses of the specimens after deformation. At room temperature (RT), the average maximum shear stress was 2050 MPa. This increased to 2304 MPa after deformation at 6 ° angle of twist at 200 °C. However, there was a decreased in the average maximum shear stress to 1564 MPa at 500 °C. These changes in the average maximum shear stresses are attributed to the effect of temperature on the microstructure and properties of the steel during deformation.

3.2. Results of dynamic impact tests

Table 2 shows the impact momentum and maximum strain rates of the room temperature and high temperature impacted Algotuf steel specimens. The specimens were all impacted at the same impact momentum of 32.35 kg · m/s.

Table 1. Strain rates and maximum shear stresses of the steel specimens after deformation.

Specimen	Angle Of Twist	Strain Rate (S^{-1})	Temperature of Test	Maximum Stress (MPa)
2	6 °	603	RT	1970
3	6 °	507	RT	1946
12	6 °	631	RT	2235
A	6 °	628	200 °C	2288
B	6 °	703	200 °C	2228
C	6 °	583	200 °C	2396
D	6 °	709	200 °C	1446
E	6 °	720	200 °C	1636
F	6 °	677	200 °C	1611

Table 2. Impact momentum and maximum strain rates of impacted specimens at room and high temperatures.

Specimen	Impact Momentum (kg · m/s)	L_O- L_F (mm)	Nominal Strain	Strain Rate (S^{-1})
00-R1 RT	32.35	1.2667	0.11965	1132
01-R2 RT	32.35	1.2650	0.11973	1133
02-R3 RT	32.35	1.2233	0.11537	1092
00-HT1-200 °C	32.35	1.1200	0.10576	1001
01-HT2-200 °C	32.35	1.0175	0.09777	925
02-HT3-200 °C	32.35	1.0325	0.09831	930
02-HT1-500 °C	32.35	1.4050	0.13311	1260
03-HT2-500 °C	32.35	1.4833	0.14029	1328
04-HT3-500 °C	32.35	1.5850	0.14932	1413

The average strain rate at room temperature was 1119 S^{-1} which decreased to 952 S^{-1} after impact at the same momentum at 200 °C. However, at 500 °C the average strain rate increased to 1334 S^{-1}.

The impact resistance graphs were similar to the true shear stress vrs shear strain graphs in the dynamic torsion tests. In response to the impact, flow stress increased initially with strain, reached a maximum and decreased with subsequent increase in strain. This trend for the flow stress was prevalent in all the impacted specimens regardless of the tests temperature as shown in Fig. 3. The amount of deformation can be approximated to be the area under the impact resistance graphs.

Table 3 shows the average yield stresses and maximum shear stresses of impacted specimens at room and high temperatures. Increasing the impact temperature decreased the average yield stress while the strain at yield increased.

3.3. Metallographic analysis on the specimens prior to and after dynamic torsion tests

The morphology of the steel specimens prior to testing consisted of large martensite laths and packets. The average hardness of the steel prior to deformation was 425 ± 14 (HV).

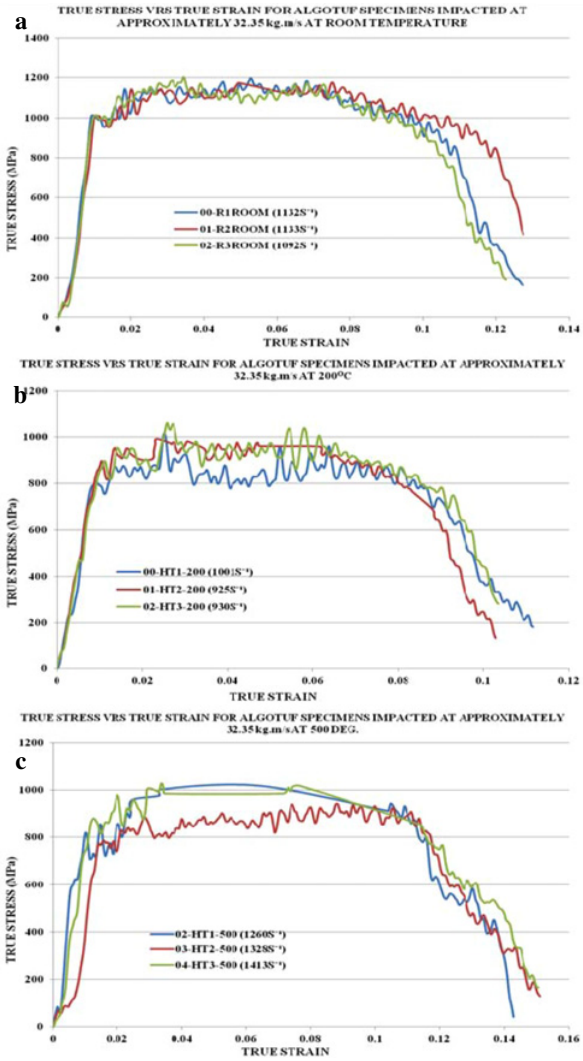

Figure 3. Impact resistance graphs of specimens impacted at 32.35 kg · m/s at (a) Room Temperature (RT), (b) 200 °C and (c) 500 °C.

Table 3. Average stresses and strains of impacted specimens.

Specimen	Yield Stress (MPa)	Yield Strain (%)	Maximum Stress (MPa)	Strain Rate (S^{-1})
00-R1 RT	1013	0.997	1162	1132
01-R2 RT	1012	0.999	1176	1133
02-R3 RT	1003	0.960	1128	1092
00-HT1-200	814	0.931	920	1001
01-HT2-200	899	1.098	960	925
02-HT3-200	880	1.065	959	930
02-HT1-500	807	1.105	1002	1260
03-HT2-500	754	1.367	916	1328
04-HT3-500	867	1.179	1011	1413

Figure 4 is a Secondary Electron Image (SEI) of the steel speceimen prior to dynamic torsion tests showing the morphology of the martensite laths. This was used as a baseline for comparison to the microstructure of the

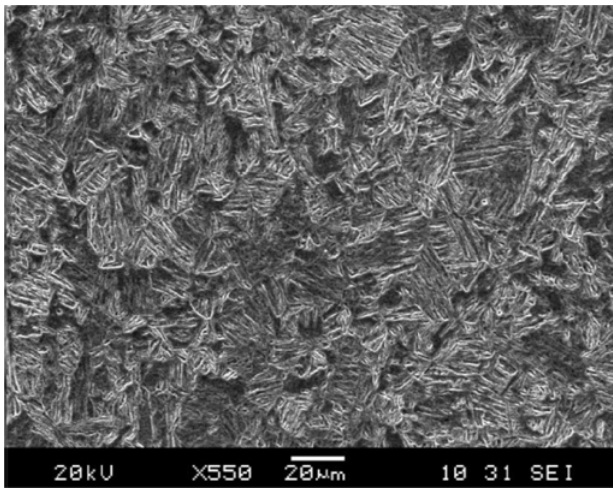

Figure 4. Scanning Electron Micrograph of Algotuf specimen prior to testing showing the morphology of the martensite laths.

deformed specimens to determine the relative degree of deformation and the changes in the microstructure that occurs after dynamic torsional testing.

Metallographic analysis on the specimen 12 after deformation at 6° angle of twist at room temperature revealed that there was no adiabatic shear band in the specimen but there was a relative increase in hardness due to the amount of deformation. There was little or no observable straining effects within the microstructure when compared to the microstructure of the untested specimens. This was predominant in all the steel specimens tested at room temperature at 6° angle of twist.

On the other hand, steel specimens that were tested at relatively higher angles of twist developed adiabatic shear bands. Figure 5 shows a crack propagating along an adiabatic shear band observed in specimen 10 which was deformed at 10° angle of twist at room temperature. The shear band leads the cracks and extensive plastic flow was observed at the tips of the cracks. The specimen fractured completely after testing. Figure 5(c) and (d) are Backscattered Electron (BSE) images that compare the structure of the shear band region to the regions surrounding the shear bands. The fine structure of the regions within the shear bands are apparent on Fig. 5(c) and (d). This is attributed to the effect of shear strain localization which results in a change from global distribution of deformation to localized distribution of deformation within the adiabatic shear bands.

No adiabatic shear band was observed in the steel specimen ddeformed at 6° angle of twist at 200°C. However, there was a relative increase in hardness compared to the untested specimen and the room temperature tested specimens due to carbide precipitation at the relatively higher deformation temperature. Figure 6 shows the Secondary Electron Image (SEI) of the steel specimen C after deformation at 6° angle of twist at 200°C showing the presence of precipitated carbides which were absent from the microstructure of the pre-deformation specimens.

At 500°C, even though the specimen did not fracture completely, there were cracks and microcracks that

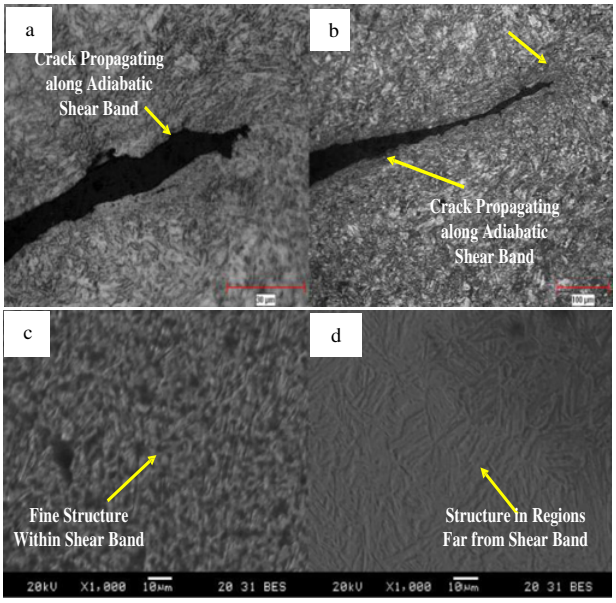

Figure 5. (a), (b) Optical micrographs of steel specimen 10 showing cracks propagating along adiabatic shear bands after deformation at 10° angle of twist at room temperature. (c) BSE micrograph of regions within the shear band (d) BSE micrograph of regions outside the shear bands.

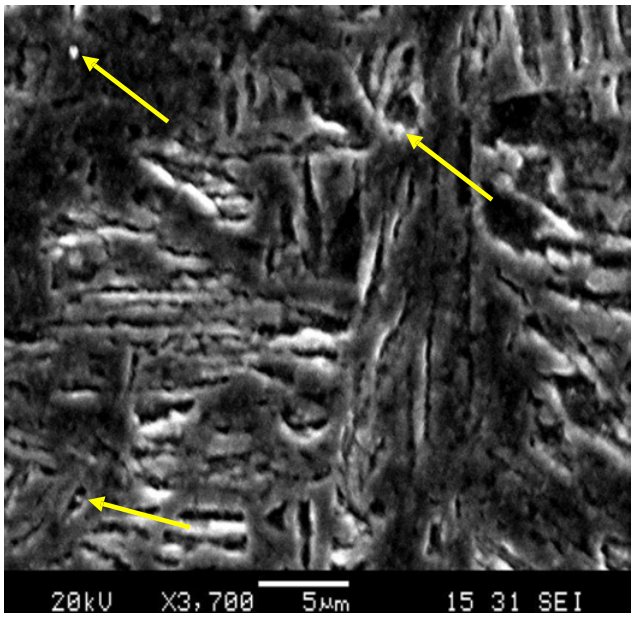

Figure 6. Scanning electron micrograph of steel specimen C showing precipitated carbides, orientation and shape of the martensite laths after deformation at 6° angle of twist at 200°C.

propagated along the length of evolved adiabatic shear bands. The testing temperature of 500°C is above the static recrystallization temperature of the steel. Testing the steel specimens at 500°C led to a significant reduction in hardness and strength due to recovery and recrystallization processes. Plastic flow in the shear bands was easily observable as shown on Fig. 7.

Average hardness measurements (HV) on the specimens prior to testing and after testing are shown on

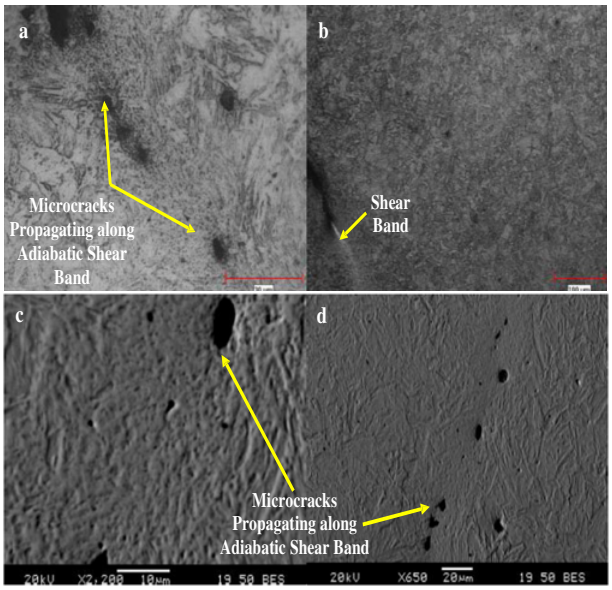

Figure 7. (a), (b) Optical micrographs (c), (d) BSE micrographs of steel specimen F showing cracks and microcracks propagating along adiabatic shear bands after deformation at 6 ° angle of twist at 500 °C.

Table 4 and Fig. 8. It was observed that hardness increased as the deformation energy increase. However, it was observed that deformation at 6 ° angle of twist at 200 °C, resulted in higher hardness and higher average maximum shear stress as was shown on Table 1. The increase in hardness and maximum shear stress is attributed to the observed precipitated carbides when the specimens were deformaed at 200 °C as shown in Fig. 8 and Table 4.

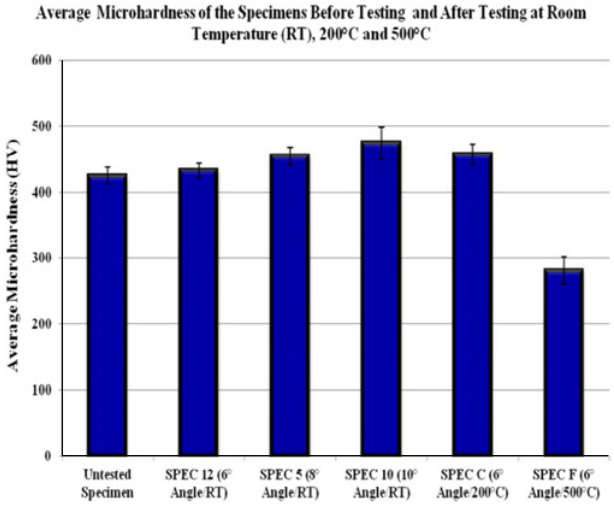

Figure 8. Average hardness (HV) for the steel specimens prior to testing and after testing at room and high temperatures.

Table 4. Average hardness distribution of the steel specimens prior to and after deformation at room and high temperatures.

Specimen	Average Microhardness (HV)
Untested Specimen	425 ± 14
SPEC 12 (6 ° Angle/RT)	433 ± 11
SPEC 5 (8 ° Angle/RT)	455 ± 13
SPEC 10 (10 ° Angle/RT)	474 ± 24
SPEC C (6 ° Angle/200 °C)	457 ± 15
SPEC F (6 ° Angle/500 °C)	281 ± 21

4. Discussions

Understanding material behaviour under large plastic strains requires measuring the strains and stresses above the tensile necking limit. A compression test and a torsion test are alternative approaches that overcome necking instability that occurs in tension tests [6].

In this study, testing the steel specimens at the same angle of twist at room temperature and high temperature revealed that prior to recrystallization, there is a relative increase in the strength of the steel specimens as well as their resistance to shear strain localization. This is evident in the steel specimen tested at 6 ° angle of twist at room temperature and at 200 °C. The strength of the steel specimens increased during the test at 200 °C which was confirmed by the increase in hardness. This is attributed to the size and distribution of the precipitated carbides. There were no carbides observed within the pre- deformation microstructure. However, at 200 °C, precipitated carbides were observed within the deformed steel specimens. It is inferred that a prior heat treatment on the Algotuf steel could increase its strength and impact resistance because of carbide precipitation. It has been reported that the prior deformation microstructure has a lot of effect on the dynamic properties and susceptibility of structural steels to shear strain localization during deformation at high strain rates and large strains [3,4]. Thus, structural steels can be heat treated to produce a strong microstructure that is resistant to strain localization during deformation at high strain rates [4].

Strain localization has been identified as a major failure mechanism in materials under high strain rates and large strains. In the current study, the dynamic impact and torsional testing on Algotuf steel specimens revealed that deformation at high strain rates and large strains causes the material to fail by the formation of narrow adiabatic shear bands (ASBs). It was observed that adiabatic shear bands preceded fracture and fragmentation leading to catastrophic failure. The higher the strain rate, the more severe the damage and the failure that occurs. Multiple shear bands with multiple cracks were prevalent in the impacted steel specimens compared to the specimens tested in torsion due to the very high strain rates that occur during impact. It is concluded that the evolution of adiabatic shear bands are the cause of damage that occurs in this steel leading to fracture and fragmentation.

5. Conclusion

In this study, two types of Hopkinson Bar systems, namely a torsional bar equipment and a direct impact system were used to test Algotuf steel specimens at room temperature (25 °C), and at high temperatures of 200 °C and 500 °C. Following the tests, the specimens were examined using optical and electron microscopy. Most of the tested specimens exhibited failure by the development of adiabatic shear bands. Some of the bands

contained microcracks which definitely confirm that the material undergoes intense plastic deformation in the shear bands before fracture occurs. This demonstrates that ASBs can serve as precursors and preferential sites for crack nucleation and propagation. Excessive grain refinement which occurs within the shear bands during impact can create potential weak points. These weak points can form microvoids which can grow and form cracks.

The financial support of Defense Research and Development Canada (DRDC DND) for this study is greatly appreciated.

References

[1] B. Dodd, and Y. Bai, Adiabatic Shear Localization: Frontiers and Advances, Elsevier (2012).

[2] Y. Xu, J. Zhang, Y. Bai, and M. A. Meyers, Shear Localization in Dynamic Deformation: Microstructural Evolution, Metallurgical And Materials Transactions A **39** (2008) 811–841.

[3] S. Boakye-Yiadom, A. K. Khan and N. Bassim, Effect of pre-impact microstructure on the nucleation and initiation of Adiabatic Shear Bands (ASBs) during impact, Materials Science and Engineering A **615** (2014) 373–394.

[4] S. Boakye-Yiadom and M. N. Bassim, Effect of prior heat treatment on the dynamic impact behavior of 4340 steel and formation of adiabatic shear bands. Materials Science and Engineering A **528** (2011) 8700–8708.

[5] M. Nabil Bassim and N. Panic, High strain rate effects on the strain of alloy steels, Journal of Materials Processing Technology $\mathbf{92 \pm 93}$ (1999) 481–485.

[6] E. Cepus, M.Sc. Thesis, University of Manitoba, Manitoba, Canada, 1995.